Effect of Mg^{2+} Ions on the Formation of Todorokite Type Manganese Oxide Octahedral Molecular Sieves

Zheng-Rong Tian,[†] Yuan-Gen Yin,[†] and Steven L. Suib*[,†,‡,§]

Department of Chemistry, Department of Chemical Engineering, and Institute of Materials Sciences, University of Connecticut, Storrs, Connecticut 06269-3060

C. L. O'Young*

Union Carbide Corporation, PO Box 8361, Technical Center, South Charleston, West Virginia 25303-0361

Received September 16, 1996. Revised Manuscript Received February 27, 1997[⊗]

The readily available permanganate, $KMnO_4$, was successfully utilized in the synthesis of manganese oxide octahedral molecular sieve (OMS-1) with the todorokite type structure. The magnesium concentration in the starting materials was systematically varied to study the synthetic chemistry of Mg−OMS-1. The techniques such as powder XRD, ICP, TGA, TPD, and redox titrations were all applied to characterize the as-synthesized Mg−OMS-1 samples. The correlation between the amount of magnesium in the starting materials and the properties of Mg−OMS-1 results in differences in (1) colors, (2) crystalline purity, and (3) thermal stabilities. Magnesium(II) ions are believed to be doped into the framework of the OMS-1 structure, but the major amount of Mg^{2+} mainly behaves as a template and is located in the tunnels of OMS-1. Two interesting Mg^{2+} concentration windows have been observed, one for the starting materials and another for the Mg^{2+} ions in the framework of Mg−OMS-1 which cover the magnesium concentration range where good quality Mg−OMS-1 can be formed.

I. Introduction

Octahedral molecular sieves (OMS), especially the porous manganese oxide type OMS materials, are raising great interest due to their potential applications not only in separations and catalysis[1−3] but also in batteries,[4−9] chemical sensors,[3] and electromagnetic materials.[10] Natural manganese oxide type OMS materials were first discovered as a major constituent of manganese nodules in the ocean. Synthetic todorokite, designated OMS-1, was made to have high thermal stability, high surface area, a well-characterized effective pore size of 6.9 Å, and novel redox properties.[1,11]

Most of the published work relating to the syntheses of manganese oxides[1,3,12] (especially Mg−OMS-1 materials) has focused more on the different properties and applications of such materials rather than on the details of the synthetic chemistry. A key parameter in these syntheses of manganese OMS-1 materials is the reagent used to oxidize Mn^{2+} to MnO_2. The original method[1] for preparation of OMS-1 relied on the use of $Mg(MnO_4)_2$, which is very expensive. That method has an advantage over the methods[12,13] involving O_2 bubbling of generation of synthetic OMS-1 materials with good crystallinity and high thermal stability (>500 °C). Therefore, an attractive modification of the $Mg(MnO_4)_2$ synthesis should involve use of less expensive reagents to make thermally stable OMS-1 phases.

The existence of a series of divalent cations such as Mg^{2+}, Co^{2+}, Ni^{2+}, Cu^{2+}, and Zn^{2+} in natural todorokite from manganese nodules of different localities and the compositional variability of natural todorokite have been observed in the literature.[14−23] Recently, a more de-

[†] Department of Chemistry.
[‡] Department of Chemical Engineering.
[§] Institute of Materials Science.
* To whom correspondence should be addressed.
[⊗] Abstract published in *Advance ACS Abstracts,* April 15, 1997.

(1) Shen, Y. F.; Zerger, R. P.; DeGuzman; R. N.; Suib, S. L.; McCurdy, L.; Potter, D. I.; O'Young, C. L. *Science* **1993**, *260*, 511−515.
(2) Bish, R. G.; Post, J. E. *Geol. Soc. Am. Abstr. Programs* **1984**, *16*, 446−625.
(3) Shen; Y. F.; Suib, S. L.; O'Young C. L. *J. Am. Chem. Soc.* **1994**, *116*, 11020−11029.
(4) Bach, B.; Periera-Ramos, J. P.; Baffier, N.; Messina, R. *Electrochim. Acta* **1991**, *36*, No. 10, 1595−1603.
(5) Strobel, P.; Charenton, J. C. *Rev. Chim. Mineral.* **1986**, *23*, 125−137.
(6) Euler, K. J.; Mueller-Helsa, H. J. *Power Sources* **1979**, *4*, 77−89.
(7) Ruetschi, P. J. *J. Electrochem. Soc.* **1984**, *131*, 2737−2744.
(8) Ruetschi, P. J.; Giovanoli, R. J. *J. Electrochem. Soc.* **1988**, *135*, 2663−2669.
(9) Voinov, M. *J. Electrochem. Soc.* **1981**, *128*, 1822−1823.
(10) DeGuzman, R. N.; Awaluddin, A.; Shen, Y. F.; Tian, Z. R.; Suib, S. L.; Ching, S.; O'Young, C. L. *Chem. Mater.* **1995**, *7*, 1286−1292.
(11) Yin, Y. G.; Xu, W. Q.; Shen, Y. F.; Suib, S. L. *Chem. Mater.* **1994**, *6*, 1803−1808.
(12) Golden, D. C.; Chen, C. C.; Dixon, J. B. *Science* **1986**, *231*, 717−719.
(13) Golden, D. C.; Chen, C. C.; Dixon, J. B. *Clays Clays Miner.* **1987**, *35*, 271−280.
(14) Burns, R. G.; Burns, V. M.; Stockman, H. W. *Am. Mineral.* **1985**, *70*, 205−208.
(15) Bunrs, R. G.; Burns, V. M.; Stockman, H. W. *Am. Mineral.* **1983**, *68*, 972−980.
(16) Burns, R. G.; Burns, V. M. *Am. Mineral.* **1978**, *63*, 827−831.
(17) Burns, R. G.; Burns, V. M. In *Marine Manganese Deposits*; Glasby, G. P., Ed.; Elsevier: New York, 1977; pp 185−248, 461−510.
(18) He, L. B *Chin. Sci. Bull.* **1991**, *36*, 1190−1193.
(19) Nimfopoulos, M. K.; Pattrick, R. D. *Miner. Mag.* **1991**, *55*, 423−434.
(20) Kokichi, I.; Sukune, T. *Kozan Chishitsu* **1989**, *39*, 205−207, 325−328.
(21) Rao, P. S.; Pattan, J. N. *Indian J. Mar. Sci.*, **1989**, *18*, 11−15.

S0897-4756(96)00478-4 CCC: $14.00

tailed study on synthetic OMS-1 samples using similar divalent cations as dopants, has been reported which results in materials with thermal stabilities around 500−600 °C, average oxidation states of manganese around 3.6 and coordination numbers of 6 for the Mn^{2+} cations.[3]

In terms of framework doping, the above-mentioned divalent cations need to be able to form six-coordinate complexes with water or framework oxygen. Studies of the correlation between stoichiometries of such divalent cation dopants in the framework and their thermal stabilities of Mg−OMS-1 would appear to be important.

Thus, to understand all of these properties and related applications of OMS-1 and to search for new types of manganese materials, structural variations and the corresponding properties of these todorokite type OMS-1 materials need to be studied. Besides, there are other driving forces for this type of research, such as the search for a cheap way to synthesize such materials, and to obtain fundamental knowledge about the limits of Mg^{2+} incorporation in todorokite type materials.

In this research we report the synthesis of OMS-1 using the inexpensive reagent $KMnO_4$ with a focus on the Mg^{2+} dopant regimes. We also investigate the stoichiometry of Mg^{2+} cations in order to study the upper and lower limits of framework substitution, tunnel Mg^{2+} contents, overall stoichiometry, crystallinity, and thermal stability. The results suggest that there is a minimum amount of Mg^{2+} ions that must be present and incorporated into the framework of OMS-1 and a maximum amount of Mg^{2+} ions that can be doped into the framework of OMS-1, to observe high purity and thermal stability.

II. Experimental Section

A. Preparation of Na−Birnessite (Na−OL-1). A layered manganese oxide material was synthesized at first according to the following procedure: 40 mL of aqueous solution was prepared to contain both $MnCl_2$ and $MgCl_2$. The $[MnCl_2]$ was fixed at 0.50 M but the $[MgCl_2]$ was varied from 0.04 to 0.70 M. While stirring this solution, 50 mL of 5.0 M NaOH was added dropwise to form a mixed slurry of $Mn(OH)_2$ and $Mg(OH)_2$, followed by the dropwise addition of 40 mL of 0.20 M $KMnO_4$ for the oxidation. After completion of this addition, the mixture was stirred for 10 more min. The resulting slurry was allowed to age at room temperature for 2 days. The supernatant liquor was then decanted and the precipitate was thoroughly washed with DDW (deionized distilled water) six times until the pH reached 7.

This washed precipitate consists of Na−birnessite, an octahedral layered (OL) material, designated as Na−OL-1. Na−OL-1 was stored in wet form before ion-exchange. The time for washing ranges from 30 min up to 3 days, depending on the $[MgCl_2]$ in the starting mixture.

B. Preparation of Mg−Buserite (Mg−OL-1) and Mg−Todorokite (Mg−OMS-1). Mg−buserite (designated as Mg−OL-1) was prepared by adding 200 mL of 1.0 M $MgCl_2$ to the Na−OL-1 formed in section II.A in a 500 mL beaker and stirred overnight at room temperature. Mg−OL-1 was washed six times with DDW followed by autoclave treatment in a 125 mL Teflon-lined stainless steel autoclave at 150 °C under autogenous pressure for 2 days. The resulting solid was filtered and washed three times with DDW followed by drying with an aspirator which led to formation of synthetic Mg−todorokite or Mg−OMS-1.

C. Inductively Coupled Plasma (ICP) Analyses. About 25−60 mg of each as-synthesized Mg−OMS-1 powder sample was weighed out and then totally dissolved in an aqueous acid solution. The inductively coupled plasma (ICP) analyses were then performed on each Mg−OMS-1 solution using a Perkin-Elmer 7-40 instrument equipped with an autosampler. A calibration check using a known standard after every 10 runs, a blank check after every five runs, and an optimization of gas flow for each sample were all applied.

D. Redox Titration. About 0.2 g of each as-synthesized Mg−OMS-1 sample was weighed out and transferred into a 250 mL Erlenmeyer flask containing a 50 mL solution of 10% H_2SO_4 mixed with 0.5 g of $Na_2C_2O_4$. With mild heating (<100 °C), this Mg−OMS-1 was dissolved completely. While the solution was hot, a 0.1 N $KMnO_4$ (standardized by $Na_2C_2O_4$ according to the standard method) was then used to back-titrate the excess $Na_2C_2O_4$.

E. XRD Studies. About 50 mg of each Mg−OL-1 and Mg−OMS-1 sample was thoroughly ground into a fine powder in an agate mortar, and then spread onto a glass slide that was mounted in a Scintag XDS-200 diffractometer. A Cu Kα radiation source was used, and the operation conditions were 45 kV, 40 mA, incident slits of 2 and 4 nm, and a step size of 0.030°.

F. Thermal Analyses. *(1) TGA.* Thermogravimetric analyses (TGA) of the as-synthesized Mg−OMS-1 samples were done with a DuPont 951 TGA instrument. About 5−10 mg of powder from each Mg−OMS-1 sample was loaded into a platinum sample holder with a carrier gas of nitrogen [UHP (ultrahigh purity) grade] flowing at 30 mL/min for all runs. The ramping rate was set at 10 °C/min with scans from 30 to 600 °C.

(2) TPD. Temperature-programmed-desorption (TPD) studies involved use of Mg−OMS-1 samples loaded into the midsection of a quartz tubular reactor (12 mm i.d. and length of 300 mm) with 60 mg of glass wool on both sides of the sample. The reactor was placed into a horizontally fixed tubular furnace (25 mm i.d. and length of 300 mm). All TPD experiments were carried out under a fixed UHP He stream of 30 mL/min and a ramping rate of 10 °C/min from 30 to 600 °C. Two liquid nitrogen coldtraps were used to remove the water evolved during heating.

A thermal conductivity detector (TCD) in a Varian Series 1400 GC was applied to monitor the oxygen evolution from the samples under heating, and an HP 3396 Series II integrator was used to quantify the signals.

III. Results

A. Changes in Color and Particle Size. As the $[MgCl_2]$ in the starting mixture increases, the color of the slurry [which is a mixture of $Mn(OH)_2$ and $Mg(OH)_2$] varies from brown to pale orange. The color variation of the oxidized slurry (Na−OL-1) is consistent with the mixed hydroxides and ranges from dark gray to gray, brownish gray, and finally to brown. Surprisingly, the color of each Na−OL-1 is the same as the color of the corresponding Mg−OL-1 and Mg−OMS-1, even after ion-exchanging and hydrothermal treatment. The higher the $[MgCl_2]$ in the starting mixture, the faster the filtration and the sedimentation of the Mg−OMS-1.

B. Elemental Analyses of Mg−OMS-1. Weight percents of K^+, Na^+, Mg^{2+}, and Mn^{2+} as a function of $[MgCl_2]$ used in the preparation, including the weight percent of oxygen/water obtained from the weight difference are given in Figures 1 and 2.

From Figure 1 one can readily note that as $[MgCl_2]$ in the starting mixture increases from 0.04 to 0.70 M, the weight percent of K^+ in the Mg−OMS-1 samples stays low (<0.1%) or is not detectable in the range 0.09−0.50 M of $[MgCl_2]$. The weight percent of Na, however, is always less than 0.2%. There is a flat stage in the

(22) Larson, T. H. *Am. Mineral.* **1962**, *47*, 59−66.
(23) Siegel, M. D. *Science* **1983**, *219*, 172−174.

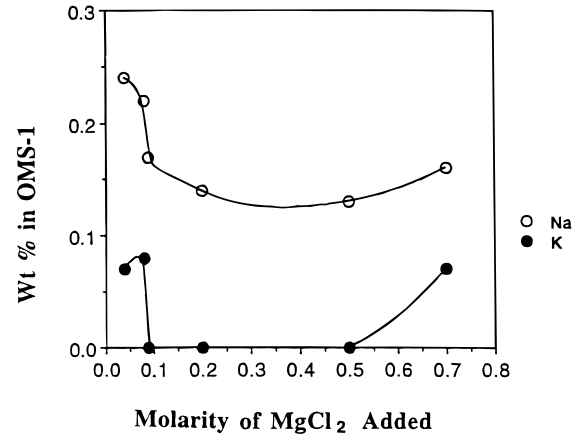

Figure 1. Potassium and sodium contents in Mg−OMS-1 vs [$MgCl_2$] in the corresponding starting mixture.

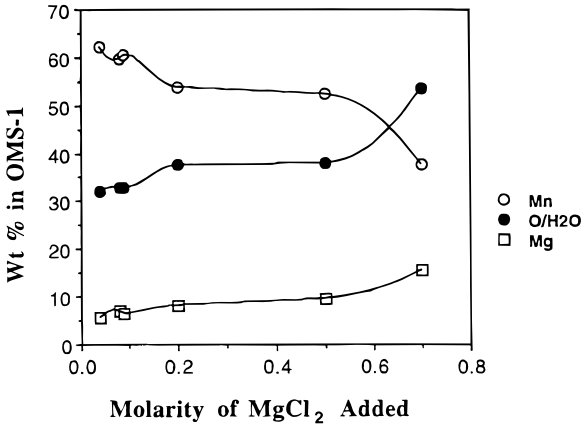

Figure 2. Weight percent for manganese, oxygen/water, and magnesium in Mg−OMS-1 vs [$MgCl_2$] in the corresponding starting mixture.

concentration profile for Na between 0.20 and 0.50 M [$MgCl_2$]. These stages represent the lowest concentrations for the sum of both K^+ and Na^+ in the autoclaved product, below and above which the concentrations of both K^+ and Na^+ in Mg−OMS-1 increase dramatically. Data from elemental analyses in Figure 2 also show a flat stage for Mg, Mn, and O/H_2O in the same range from 0.20 to 0.50 M of [$MgCl_2$], which mimic the trends for Na.

The Mg weight percent in the OMS-1 gradually increases from 5.46% for 0.04 M to 7.08% for 0.08 M, then drops to 6.51% for 0.09 M, then stays almost the same from 8.14% for 0.20 M to 9.57% for 0.50 M, and then increases quickly to 15.64% for 0.70 M [$MgCl_2$] as shown in Figure 2.

The Mn weight percent decreases slightly from 62.47% at 0.04 M to 52.38% at 0.08 M, then to 37.71% at 0.09 M, and then decreases to 53.93% at 0.20 M, stays flat until 0.50 M, and then decreases to 37.71% at 0.70 M of [$MgCl_2$]. This trend is consistent with the change in weight percent for Mg (or, more Mg, less Mn) in the solid Mg−OMS-1 sample.

The weight percent of total oxygen plus water (O/H_2O) varies from 31.96% for 0.04 M to 33.03% for 0.08 M, then is 32.91% for 0.09 M, and then increases to 37.52% for 0.20 M of [$MgCl_2$]. Thereafter, the amount of 37.92% for 0.50 M is about the same, finally increasing to 53.58% for 0.70 M of [$MgCl_2$]. It is an interesting phenomenon that the concentration profiles for Mg and O/H_2O are very similar.

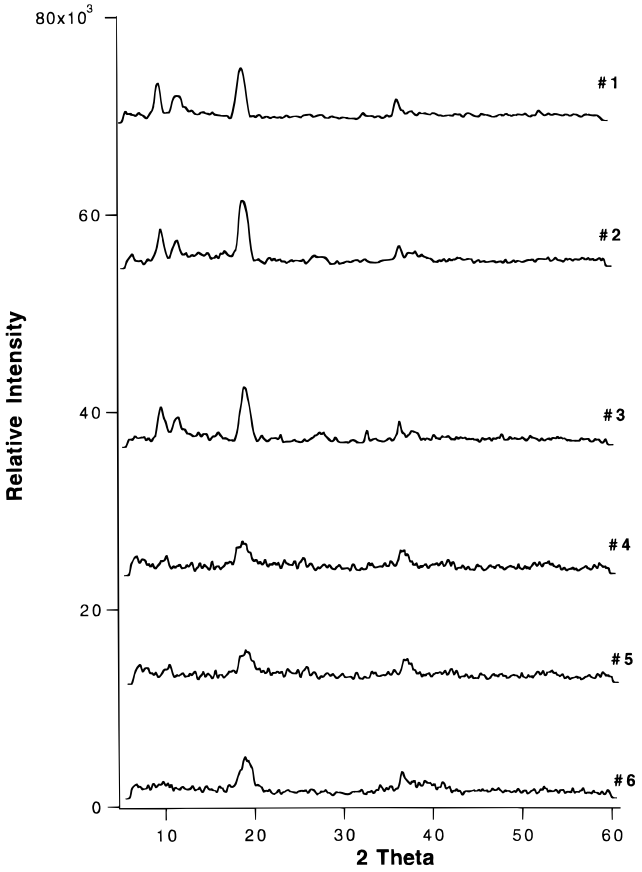

Figure 3. XRD patterns for Mg−OL-1 samples. (1) 0.04 M [$MgCl_2$] in the starting mixture. (2) 0.08 M [$MgCl_2$] in the starting mixture. (3) 0.09 M [$MgCl_2$] in the starting mixture. (4) 0.20 M [$MgCl_2$] in the starting mixture. (5) 0.50 M [$MgCl_2$] in the starting mixture. (6) 0.70 M [$MgCl_2$] in the starting mixture.

These weight percent change profiles (for K, Na, Mg, Mn, and lattice oxygen plus tunnel water) are all unique for samples of 0.20 and 0.50 M [$MgCl_2$] which represent turning points in the synthesis. These turning points may be related to changes in structure (vide infra) or fortuitous. The flat regions in Figures 1 and 2 may represent a $MgCl_2$ concentration "window" within which only the same phase (OMS-1) could be prepared.

C. XRD of Mg−OL-1 and Mg−OMS-1. The XRD patterns of all Mg−OL-1 samples are displayed in Figure 3. The highest *d* spacing peak of 9.6 Å (100) is the diagnostic peak for Mg−OL-1. Sample 5 (0.50 M [$MgCl_2$] added before precipitation in the synthesis) represents a $MgCl_2$ concentration boundary. Mg−OL-1 is observed in sample 5 but not observed in sample 6. The second highest *d* spacing peak starts to grow on the right side of the 9.6 Å peak in samples from 3 (0.09 M [$MgCl_2$]) to 1 (0.04 M [$MgCl_2$]). This extra broad peak has a *d* spacing around 8.2 Å that is between the 9.6 Å peak for buserite and the 7.0 Å peak for birnessite.

The XRD patterns of autoclaved Mg−OMS-1 samples in Figure 4 have similar systematic trends. Sample 5 (Mg−OMS-1) once again behaves as an indicator of the key [$MgCl_2$] needed in the synthesis of pure Mg−OMS-1. More [$MgCl_2$] (as in sample 6) makes it difficult to form a good crystalline phase of Mg−OMS-1, but less [$MgCl_2$] allows the formation of Mg−OMS-1. Instead of observing the 8.2 Å peak as in Mg−OL-1, the corresponding Mg−OMS-1 sample has an intense peak

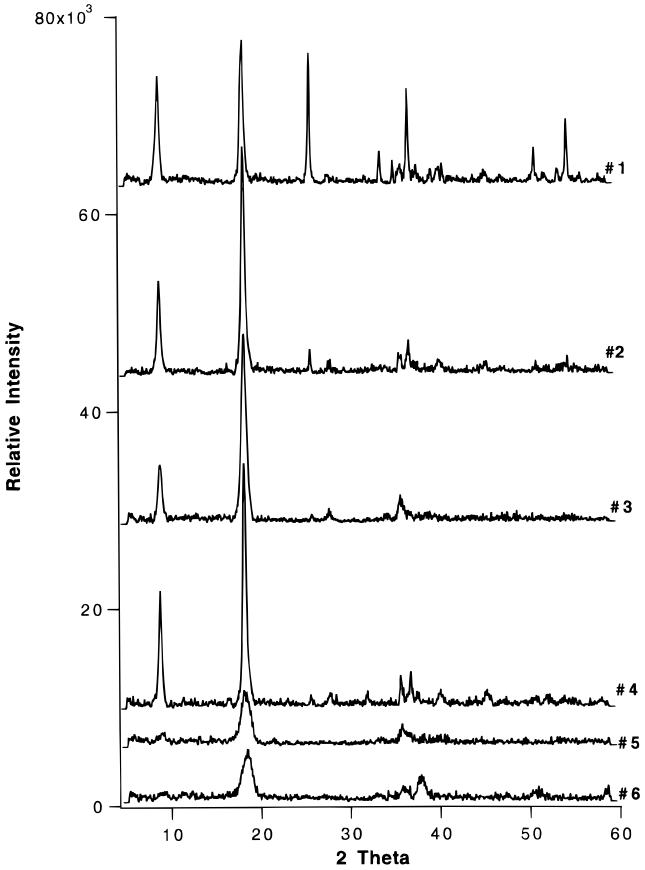

Figure 4. XRD patterns for Mg−OMS-1 samples. (1) 0.04 M [$MgCl_2$] in the starting mixture. (2) 0.08 M [$MgCl_2$] in the starting mixture. (3) 0.09 M [$MgCl_2$] in the starting mixture. (4) 0.20 M [$MgCl_2$] in the starting mixture. (5) 0.50 M [$MgCl_2$] in the starting mixture. (6) 0.70 M [$MgCl_2$] in the starting mixture.

positioned at $2\theta = 26.2°$ or 3.4 Å *d* spacing. This peak for the intermediate phase with *d* spacing 3.4 Å was observed first as a weak peak in sample 3 and then as a strong peak in sample 1 as shown in Figure 4.

D. Average Oxidation State. The $KMnO_4$ solution was standardized to be 0.0843 M with a relative error of 0.24% in the titration. On the basis of results from XRD and elemental analyses, two samples (samples 4 and 5) were chosen for redox titration to cover the range where pure OMS-1 phase can form. The average oxidation state of sample 4 is 3.43(+) and the average oxidation state of sample 5 is 3.36(+), with a relative error of titration less than 1% for both samples.

E. TGA and TPD. *(1) TGA.* Derivatives of the weight loss data of TGA give rise to the peaklike DTGA data which are easy for recognition and are displayed with the TGA data in the same figures. The weight losses in TGA data of Figure 5 are due to either water or oxygen. All autoclaved Mg−OMS-1 samples have a fairly large weight loss, ranging from ∼10% for the sample 1 to ∼20% for sample 6 at about 300 °C as shown in the TGA/DTGA figures. The more $MgCl_2$ added in the starting mixture leads to larger weight loss at about 300 °C for the final products (Mg−OMS-1). Distinguishing water from oxygen has been accomplished with a combination of TGA/DTGA and TPD results described later in this work.

As the [$MgCl_2$] in the starting mixture increases, the second major peak of weight loss in the DTGA data near 500−520 °C decreases from 4% in sample 1 to 2% in sample 4, then becomes difficult to be observed in sample 5, and does not exist in sample 6. These data suggest that sample 6 may be totally different from the rest of the autoclaved samples, which agrees very well with the XRD results for the Mg−OMS-1 samples.

In addition, another minor weight loss appears around 420 °C. In the DTGA data there is a peak at 420 °C for sample 1, then changes to a tiny ripple in sample #4, is hard to identify in sample 5 and disappears in sample 6. Once again this trend suggests that sample 5 is a turning point of [$MgCl_2$] in the syntheses of OMS-1 materials.

There is another informative trend in these TGA/DTGA data around 200 °C or below. As the [$MgCl_2$] in the starting mixture increases, the number of weight loss peaks near and below 200 °C increases. The larger number of peaks in this range may be due to more functional groups, impurities or other phases present in the Mg−OMS-1 materials.

(2) TPD. The TPD data of Figure 6 show amounts of oxygen released from the as-synthesized OMS-1 samples. These samples (5, 3, 2, and 1) were selectively chosen to cover the range of the samples believed to contain Mg−OMS-1 based on experimental XRD and TGA/DTGA data.

Almost all the samples tested by TPD evolve lattice oxygen at high temperature around 550 °C, with the trend that the higher [$MgCl_2$] in the starting materials results in smaller peaks for oxygen evolution at this high temperature but more numbers of peaks at lower temperatures. In other words, more and more kinds of relatively active oxygen species are evolved at relatively lower temperature in high Mg content samples. No large peak for O_2 evolution was found at 300 °C, which was the temperature observed in TGA/DTGA data that show large weight losses for all Mg−OMS-1 samples.

The surface areas of these OMS-1 materials range from about 100 to about 250 m^2/g. These data clearly show that these materials are porous. For transition-metal oxide systems such as these it should be realized that the surface areas by definition are inherently smaller than materials with lower atomic weights of elements such as Si, Al such as in silica, alumina, and zeolites. Adsorption data for these systems show uptakes on the order of 20 g of adsorbate/100 g of OMS-1 for adsorbates smaller than 6.9 Å.

IV. Discussion

The hydroxides of Mg(II) and Mn(II) have the same CdI_2 type structure in which the Mg^{2+} and Mn^{2+} ions are surrounded by six OH^- groups to form a layered structure.[24] This geometry is very stable for $Mn(OH)_2$ and brucite [$Mg(OH)_2$] materials.

Since the ionic radii of Mg^{2+} (0.86 Å) and of Mn^{2+} (0.81 Å) are so close,[25] clusters of $Mg(OH)_6^{4-}$ and $Mn(OH)_6^{4-}$ should also be similar in size. When two hydroxides form at the same time, a certain amount of magnesium hydroxide would likely enter the framework

(24) Wells, A. F. *Structural Inorganic Chemistry*, 4th ed.; Clarendon Press: Oxford, 1975; pp 209−210, 520−521.
(25) Evans, H. T., Jr. *Ionic Radii in Crystals, CRC Handbook of Physics and Chemistry*, 73rd ed.; CRC Press: Boca Raton, FL, 1992; p 12−8.

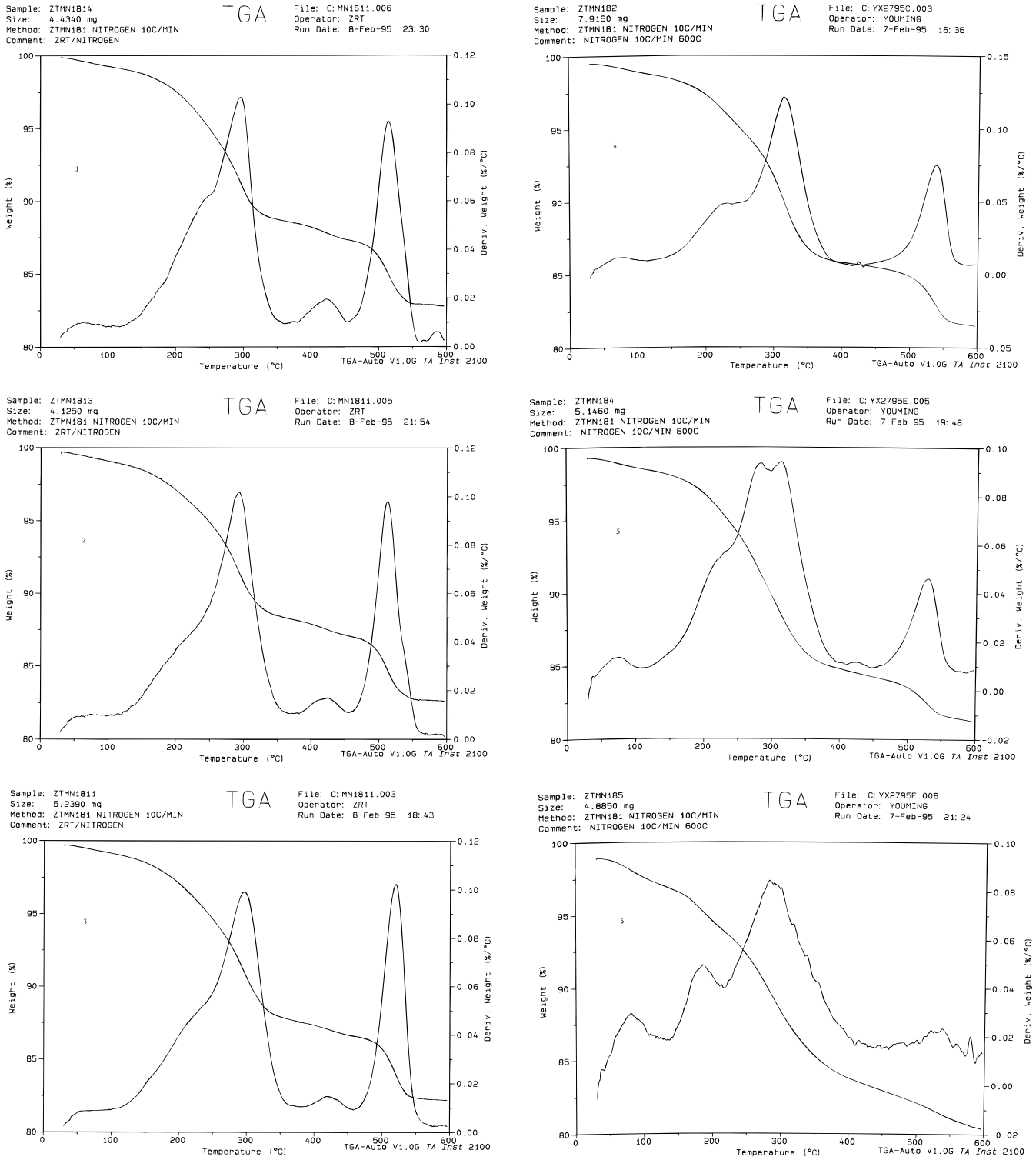

Figure 5. Thermogravimetric analyses (TGA) for Mg−OMS-1 samples. (1) 0.04 M [$MgCl_2$] in the starting mixture. (2) 0.08 M [$MgCl_2$] in the starting mixture. (3) 0.09 M [$MgCl_2$] in the starting mixture. (4) 0.20 M [$MgCl_2$] in the starting mixture. (5) 0.50 M [$MgCl_2$] in the starting mixture. (6) 0.70 M [$MgCl_2$] in the starting mixture.

of manganous hydroxide to form a good mixture such as $[Mn(OH)_2]\cdot[Mg(OH)_2]_y$ where $(1 < y < 0)$.

After the oxidation by $KMnO_4$, $Mn(OH)_2$ was readily transformed to MnO_2 with the structure of birnessite (OL-1) which is similar to that of $Mn(OH)_2$. At this stage Mg^{2+} ions would still most likely stay in framework positions as before the oxidation. The substitution of Mg^{2+} in octahedral sites of birnessite (OL-1) is not surprising. In fact, Mg^{2+} substitution in layered materials also occurs for octahedral Al^{3+} sites such as in montmorillite, illite, chlorite, and vermiculite clays.

The replacement of Mn^{4+} ions (by Mg^{2+}, Mn^{3+}, or even Mn^{2+}) in the framework of OL-1 requires other cations to satisfy the charge balance unless defects such as oxygen vacancies occur. As the amount of $MgCl_2$ in the starting mixture increases, MgO_6^{4-} clusters can occupy more and more positions of MnO_6^{2-} and MnO_6^{3-} in OL-1. Therefore, more and more types of oxygen defects can develop.

A. Colors and Oxidation States. The differences between the samples of darker color and of lighter color, for all Na−OL-1, Mg−OL-1, and Mg−OMS-1 materials

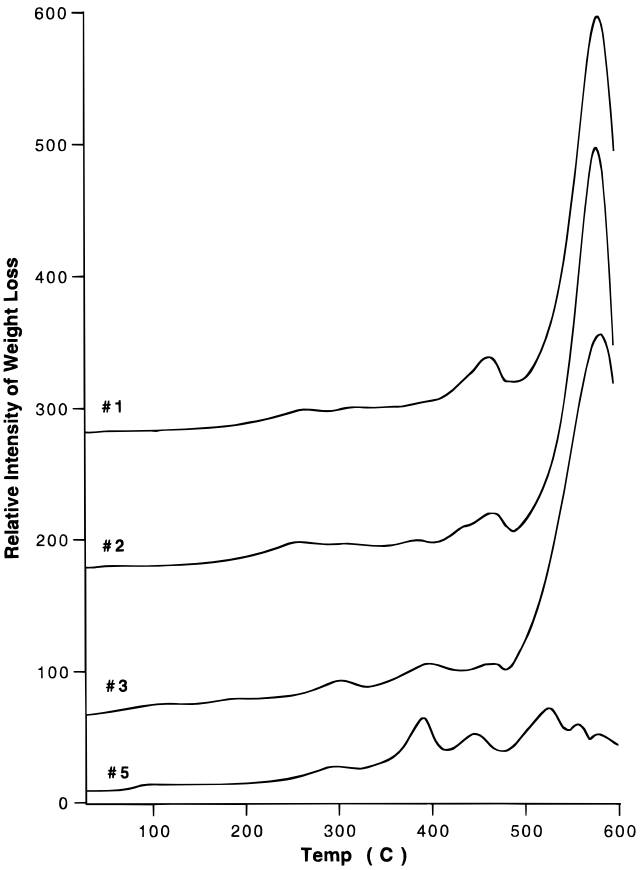

Figure 6. Oxygen TPD spectra for Mg−OMS-1 samples. (1) 0.04 M [$MgCl_2$] in the starting mixture. (2) 0.08 M [$MgCl_2$] in the starting mixture. (3) 0.09 M [$MgCl_2$] in the starting mixture. (5) 0.50 M [$MgCl_2$] in the starting mixture.

are due to a difference in average oxidation states related to the amounts of Mg^{2+} in the solid samples. In general, mixed valency corresponds to a dark color.[26] Here, the different mixed valences (or different average oxidation states) must be responsible for the color variations in the Na−OL-1, Mg−OL-1, and Mg−OMS-1 samples.

Since MnO_2(IV) is gray and Mn_2O_3(III) brown, it is understandable that the lower the average oxidation state, the more the brown color, or the more Mn^{3+} ions in the corresponding Mg−OMS-1 material. Furthermore, the identity in color for Na−OL-1, for the corresponding Mg−OL-1, and corresponding Mg−OMS-1 materials suggests that the average oxidation state does not change much during the ion-exchange and the autoclave treatment.

According to the ratio for Mn(VII)/Mn(II) of 2/7 in the starting materials, the final oxidation state of Mn must be 3.8(+). However, the observed average oxidation state is in fact 3.43(+) for sample 4 and 3.36(+) for sample 5 which is consistent with another observation that sample 4 is gray and sample 5 dark brown. These obvious differences in average oxidation state and color suggest that more Mg^{2+} ions (as in sample 5) in the framework (discussed in later sections) must cause more oxygen defects. In consequence, these defects are in fact active oxygen species which can easily leave as free O_2 to lower the average oxidation state of Mn (or more Mn^{3+} ions formed as reflected by more brown color for solid) in the framework. Other TPD studies of OMS-1 materials are consistent with this suggestion.[6]

B. XRD. The systematic structural changes for the as-synthesized final products are consistent with the amounts of Mg^{2+} cations added in the starting materials. This is in line with the above discussion of framework Mg^{2+} cations and their role in the formation of tunnel-like OMS-1 materials. Since the 9.6 and 4.9 Å *d* spacing lines in the diffraction patterns serve as two diagnostic peaks for the OMS-1 phase,[15] it is hard to believe that samples, like sample 6 (0.70 M [$MgCl_2$] in the starting mixture), that lack this 9.6 Å peak in the XRD pattern of the autoclaved product are authentic OMS-1 materials.

At the other extreme, too few Mg^{2+} cations can force impurities to be incorporated into Mg−OMS-1. If the [$MgCl_2$] decreases to 0.09 M as in sample 3, the XRD patterns for OL-1 developed a new peak at a *d* spacing of 8.2 Å. Neither OMS-1 nor OL-1 should contain this new peak at 8.2 Å. None of the XRD patterns for pure OMS-1, however, have this 8.2 Å peak. A new peak with *d* spacing 3.38 Å (in samples 1−3) in Figure 4 matches the third strongest peak at 3.34 Å (241) of buserite. It is clear then that the foreign phase represented by the 8.2 Å peak in impure Mg−OL-1 is responsible for the buserite peak at 3.34 Å in the impure OMS-1 materials. The phase containing the 8.2 Å peak is a new intermediate phase between Na−OL-1 and Mg−OL-1 due to an insufficient amount of Mg^{2+} cations in the framework, and this intermediate phase is readily transformed to buserite after autoclave treatment.

Therefore, "window-1" for [$MgCl_2$] in the starting materials spans from 0.40 (0.20 M/0.50 M) Mg/Mn ratio for sample 4 to 1.0 (0.50 M/0.50 M) for sample 5. We have only been able to prepare pure Mg−OMS-1 within this window-1.

C. Chemical Analyses. The chemical analyses from ICP revealed significant information for understanding the role of magnesium in the formation of OL-1 and OMS-1 structures. The complete ion-exchange (as reflected by the Na^+ content less than 0.2% and K^+ content not detectable) indicates that almost all tunnel cations are Mg^{2+} ions or almost all Mn cations are present in the framework. Within the above-mentioned window-1, the resulting final oxidation state of Mn in sample 5 is about 3.36(+), which suggests that every two Mn cations [6.72(+)] in the OMS-1 materials must create a deficiency of 1.28 (8 − 6.72 = 1.28) positive charges with respect to the Mn^{4+}. Therefore, we can deduce that every 200 Mn cations in the framework must generate 128 unbalanced negative charges that need only 64 Mg^{2+} cations in the tunnel for charge compensation. If the total oxidation state of Mn and the total amount of Mn are both known, the amount of this type (T-type) of Mg^{2+} cations in the tunnels must also be fixed. The ratio of this T-type tunnel Mg^{2+} cations to the total amount of Mn cations must be 64/200.

In accordance with the results of Figure 2, the ratio of Mg/Mn is 0.42 for sample 5. On the basis of considerations of the highest Mg/Mn molar ratio of 0.42 in pure crystalline OMS-1 materials for sample 5; the fact that each tunnel Mg^{2+} ion will compensate two unbalanced charges caused by four Mn cations (two

(26) West, A. R. *Basic Solid State Chemistry*; John Wiley & Sons: New York, 1988; pp 297−299.

Mn^{3+} and two Mn^{4+}) in the framework; the total oxidation state and the total amount of Mn in the resultant materials, there is no way that all Mg^{2+} cations are present in the tunnels (T) for neutralization of unbalanced framework (F) charges only caused by mixed valency in Mn. Instead, a certain percent of the Mg^{2+} cations must enter the framework of OMS-1 resulting in some unbalanced charges in this framework.

From the above-mentioned Mg/Mn ratios for sample 5 (0.42 as the total Mg content in OMS-1, and 64/200 as the content of T-type Mg^{2+} cations required in the tunnel to balance the charge of Mn), simple subtraction tells us that Mg/Mn ratio of 0.10 ($0.42 - 64/200 = 0.10$) must be the content of other types of Mg^{2+} cations. These Mg^{2+} ions must be split into two types, one half as T-type in the tunnel sites to neutralize the unbalanced charges caused by the other half of F-type Mg^{2+} cations in the framework (F), because each Mg^{2+} in the framework creates two unbalanced charges with respect to the Mn^{4+}. Thus, the highest framework doping ratio of Mg/Mn or highest concentration of F-type Mg^{2+} cations in the OMS-1 framework must be one half of 0.10, or 0.050 or 5.0%. This number of 5.0% represents the upper limit of substitution in the framework of Mg−OMS-1 or could be called a framework saturation limit. In other words, the framework saturation limit of Mg^{2+} ions in Mg−OMS-1 must be close to 0.050 of the Mg/Mn ratio.

In the same manner, we can deduce that sample 4 [with an overall Mg/Mn ratio of 0.34 and total oxidation state of 3.43(+)] in the solid has the lowest framework doping limit of 0.030 or 3.0% of the Mg/Mn ratio. It is quite interesting that the F-type Mg^{2+} content needs to be at least 0.030 in the ratio of Mg/Mn if a pure Mg−OMS-1 phase is desired.

It is clear that Mg^{2+} ions in the Mg−OMS-1 framework must be somewhere between the Mg/Mn ratio of 3.0% and 5.0%. This short range acts as a narrow "window-2" of allowable Mg^{2+} contents in the framework of Mg−OMS-1.

If [$MgCl_2$] in the starting materials is larger than 0.70 M, the Mg^{2+} cations have to occupy other sites in the framework. This would create more defects with more unbalanced charges making it difficult to form the OMS-1 tunnel-like framework, as observed in the XRD patterns of Figure 4.

The data of Figures 1 and 2 also suggest that the concentration of each element in Mg−OMS-1 is relatively unchanged within this window range of 0.20 and 0.50 M of [$MgCl_2$], as reflected by the flat stages in the weight percent profiles. This implies that pure Mg−OMS-1 must have a relatively fixed formula in which the Mg/Mn ratio can only vary from 0.34 for sample 4 to 0.42 for sample 5.

For sample 5, the Mg/Mn ratio in the starting mixture is 1.0, and in the framework of the corresponding final product is 0.05. The difference between these two ratios suggests that with a high [$MgCl_2$] of 0.5 M at most 5 of every 100 (0.050/1.0 or 5.0%) Mg^{2+} cations in the solution of starting mixture can enter the framework of the OMS-1 final product.

The lower limit to form pure Mg−OMS-1 is at a Mg/Mn ratio of 0.40 for the starting mixture and at a Mg/Mn ratio of 0.030 for the framework of the corresponding OMS-1 material (sample 4). The difference between these two lower limits suggests that with a low [$MgCl_2$] of 0.20 M, at least three of every 40 (0.030/0.40 or 7.5%) Mg^{2+} cations in solution must enter the framework of OMS-1 in order to form pure Mg−OMS-1.

The mole fraction of F-type Mg^{2+} ions to the total Mg^{2+} ions can also be established. It is 0.030/0.34 or about 8.8% for sample 4 and 0.050/0.42 or 12% for sample 5. This is to say that about 9−12% of Mg^{2+} ions are in the framework of Mg−OMS-1 and about 89−92% of Mg^{2+} ions are in the tunnels of Mg−OMS-1.

The very low levels of K^+ and Na^+ (believed to occupy the very few tunnel sites of OMS-1) suggest that the time of overnight stirring must be long enough to complete the ion-exchange. A high-quality Mg−OMS-1 sample with nearly 0% K^+ cations suggests that the K^+ content is lower than the ICP detection limit which can be used as a marker of the purity of Mg−OMS-1. The very low level of Na^+ content may be caused by either the difficulty in removal of all monovalent Na^+ cations during ion-exchange by Mg^{2+} or the necessity for some sites in the tunnel to allow only monovalent cations.

A reviewer has suggested that the conclusion about the presence of magnesium ions in the framework, oxygen defects, and thermal stability (vide infra) are speculative. The speculation is a result primarily of elemental analyses, redox titration data, and other experiments. It is clear that a better understanding of the structural features of these materials is needed in order to obtain better evidence of Mg^{2+} framework substitution.

D. Thermal Analyses. The TGA/DTGA data represent the weight losses of both water and oxygen, but TPD shows only evolved oxygen. The weight loss at each temperature due to either oxygen or water can readily be distinguished by the comparision of TGA/DTGA and TPD.

The weight loss at temperatures ranging from 280 to 320 °C is due to water evolution, and the one starting to appear near 500−520 °C must be due to lattice oxygen evolved from OMS-1 on the basis of TGA/DTGA and TPD data. The Mg−OMS-1 samples evolve water around 300 °C, but not lattice oxygen until the temperature is above 500 °C. These data are consistent with thermal properties of OMS-1 reported elsewhere.[1,3] It is clear that our Mg−OMS-1 samples start to decompose at temperatures above 500 °C, which is consistent with the result of using $Mg(MnO_4)_2$.[1]

Another small weight loss at 420 °C in DTGA (not observed in TPD) is definitely due to weight loss of water and is observed only for samples 1−3, which may be due to another phase besides OMS-1. Since samples 1−3 (discussed early) are believed to have some unconverted buserite phase, it is suggested that the weight loss at 420 °C is due to this unconverted buserite, and the relatively small peak intensity in the DTGA suggests that the buserite phase in these OMS-1 samples is really only a minor component.

The other trend in the TPD spectra is that more oxygen evolution peaks exist at lower temperature for the samples with more Mg^{2+} ions in the framework. An increase in the content of Mg^{2+} ions in the framework leads to a lower thermal stability for the Mg−OMS-1. This also has proved a good correlation between the Mg^{2+} concentration in the framework of OMS-1 (or the

amount of oxygen defects) and the thermal stability of these OMS-1 samples. This correlation supports our suggestion that Mg^{2+} in the framework of OMS-1 samples plays a critical role in the synthesis of Mg−OMS-1 materials.

V. Conclusions

In the synthesis of todorokite type OMS-1 materials, taking into consideration the $Mg(OH)_2$ and $Mn(OH)_2$ structures, certain amounts of Mg^{2+} ions in the framework are essential for the formation of pure and thermally stable Mg−OMS-1 with good crystallinity. The colors, average oxidation states, purities and crystallinities of Mg−OMS-1 phases are all very sensitive to how much Mg^{2+} is present in the framework of Mg−OMS-1.

The inexpensive $KMnO_4$ can be used for substituting the expensive $Mg(MnO_4)_2$ to make similar thermally stable Mg−OMS-1 materials if the proper concentrations of Mg and Mn in the starting materials are selected.

For the preparation of pure Mg−OMS-1 phase, the $[Mg^{2+}]$ in the starting material should fall into the window-1 range of 0.34−0.42 in the ratio of Mg/Mn. For the formation of good quality Mg−OMS-1, the Mg^{2+} content in the framework must fall into the window-2 range of 0.030−0.050 in the ratio of Mg/Mn. The pure Mg−OMS-1 samples have only about 9−12% of F-type Mg^{2+} ions existing on the framework, the other 89−92% of T-type Mg^{2+} ions are in the tunnels of Mg−OMS-1 as templates.

Changes in color and average oxidation state are all sensitive to the Mg^{2+} content in the framework of Mg−OMS-1. The difference of only 3% in Mg/Mn ratio for the framework Mg^{2+} contents between samples 4 and 5 is responsible for the obvious changes in average oxidation state (3.43 and 3.36, respectively) and color (grayish brown and brown, respectively).

Thermal stabilities of these OMS-1 samples also depend upon the concentration of Mg^{2+} or the concentration of defects in the framework of Mg−OMS-1. In general, as the framework concentrations of Mg^{2+} ions increase, the Mg−OMS-1 samples start to decompose at lower and lower temperatures. The temperature of 530 °C is the upper limit at which our Mg−OMS-1 samples can be stable. Further studies are underway to study the chemical environments of Mg^{2+} ions in the framework and more direct determination of framework Mg^{2+} content, which are expected to be important for understanding the applications of Mg−OMS-1 type materials.

Acknowledgment. We acknowledge the U.S. Department of Energy, Office of Basic Science, Division of Chemical Sciences and Texaco, Inc. for the support of this research.

CM960478V